Check for updates

Smart capsule for non-invasive sampling and studying of the gastrointestinal microbiome†

Jose Fernando Waimin, ‡[ab] Sina Nejati, ‡[ab] Hongjie Jiang, [bcd] Jake Qiu,[be] Jianghsan Wang,[be] Mohit S. Verma[bef] and Rahim Rahimi ⋆[abc]

Gut microbiota plays an important role in host physiology such as obesity, diabetes, and various neurological diseases. Thus, microbiome sampling is a fundamental approach towards better understanding of possible diseases. However, conventional sampling methods, such as endoscopies or colonoscopies, are invasive and cannot reach the entire small intestine. To address this need, a battery-less 3D-printed sampling capsule, which can collect microbiome samples throughout the entirety of the GI tract was designed. The capsule (9 mm × 15 mm) consists of a 3D printed acrylic housing, a fast-absorbing hydrogel, and a flexible PDMS membrane. Fluids containing samples of the microbial flora within the GI tract enter the device through a sampling aperture on the cap of the device. Once the microbiome enters the housing, the hydrogel absorbs the fluid and swells, effectively protecting the samples within its polymeric matrix, while also pushing on the flexible PDMS membrane to block the sampling aperture from further fluid exchange. The retrieved capsule can be readily disassembled due to the screw-cap design of the capsule and the hydrogel can be removed for further bacterial culture and analysis. As a proof of concept, the capsule's bacterial sampling efficiency and the ability to host microbial samples within the hydrogel in a sealed capsule were validated using a liquid culture containing *Escherichia coli*. The demonstrated technology provides a promising inexpensive tool for direct sampling and assessment of microbes throughout the GI tract and can enable new insights into the role of diet in mediating host–microbe interactions and metabolism.

Introduction

Over the past decade, there has been a tremendous surge in research focused on the human microbiome. The findings from this research have had a profound impact on our understanding of the vast and diverse microorganisms found in the human gut and the vital role that they play in the pathophysiology which dominates human health. Many of these studies have identified the effects of the gut microbiota on human metabolism, nutrition uptake, efficacy of orally-administered therapeutics, and functionality of immune and neural systems. For example, a number of studies have found correlations between

microbiota imbalance (dysbiosis) and various diseases including diabetes, obesity, and metabolic syndrome; diseases which affect approximately 30 million people in the US.[1–6] Similarly, new insights regarding possible ways that gut bacteria may influence development and maintenance of the nervous system, suggest a link between gut microbiome composition and the regulation of psychoneurological disorders including anxiety, depression, and dysbiosis in autism.[7–10] Furthermore, studies have also shown that the presence of specific bacterial species can alter the metabolism of certain drugs, such as chemotherapeutic agents and antiviral drugs. Not only biotransformation of certain drugs can cause drug-related toxicities, it can also provide a mechanism by which drug developers could exploit host microbiota to create more site-specific drug delivery. Therefore, human microbiome sampling is essential to understand the mechanisms of microbiota–drug interactions as well as the degree to which this complex interplay can affect the drug efficacy and bioavailability. Much of what is known regarding the structure and function of the human gut microbiome have been ascertained from *ex situ* culturing and/or sequencing of bacteria from fecal samples. In fact, since only a small fraction of gut bacteria is available and culturable from fecal samples, major efforts have been conducted in utilizing tools that will enable direct

[a]School of Materials Engineering, Purdue University, West Lafayette, Indiana, 47907, USA. E-mail: rrahimi@purdue.edu

[b]Birck Nanotechnology Center, Purdue University, West Lafayette, IN 47907, USA

[c]School of Electrical Engineering, Purdue University, West Lafayette, Indiana, 47907, USA

[d]Shenzhen MSU-BIT University, Shenzhen, Guangdong, China

[e]Department of Agricultural and Biological Engineering, Purdue University, West Lafayette, IN 47907, USA

[f]Weldon School of Biomedical, Purdue University, West Lafayette, IN 47907, USA

† Electronic supplementary information (ESI) available. See DOI: 10.1039/c9ra10986b

‡ These authors contributed equally to this work.

sampling of microorganisms from the entire GI tract. However, direct sampling from the GI tract has numerous challenges owing to its long length (9 m) and diameter alterations.[11] While different colonoscopy and gastroscopy sampling methods are currently used, they are limited to sampling at certain sections throughout the GI tract and are invasive approaches which cause patient discomfort and can lead to decreased compliance.[12–14] As an alternative approach, smart functional capsules with the ability to collect samples at different targeted locations in the entire GI tract can address several limitations associated with conventional colonoscopy and gastroscopy.[15,16] Furthermore, capsule-based devices can improve patient comfort, without the requirement of being administered in clinical settings. Perhaps one of the best-known smart capsules used for diagnostic and treatment in the field of gastrointestinal disorder is the PillCam™ capsule endoscopy (CE) technology. It is widely used as the gold standard for collecting images from hard-to-reach areas throughout the GI tract. It is estimated that more than 2 million CEs have been used over the past 15 years to diagnose diseases related to the small intestine, such as obscure GI bleeding, tumors, Crohn's disease, angiodysplasia, celiac disease, and polyposis.[12,14,16–18] However, despite the great imaging diagnostic capabilities of the PillCam technology, its main drawback is its lack of ability to collect and store samples inside the pill as it travels through the GI tract. Over the past decade there have been several efforts in developing new smart capsules with different sampling methods that can be classified into two main categories of active and passive devices. In active devices, the actuation and sampling mechanism are often attained by using an on-board battery that provides the required energy to actuate various plungers, pistons, and biopsy forceps.[15,19–21] For instance, Park et al. designed an active capsule that takes tissue biopsies with a microactuator that moves forward and backward via slider-crank mechanism.[20] The triggering process of microactuator is achieved by electric power applied to the shape memory alloy heating wire. In another study, by Cui et al., a capsule was designed to push the drug out of a piston while simultaneously sucking sampling fluid into the reservoir.[22] The actuation mechanisms were driven by an on-board battery which was considered as the largest component in the device.[16] Battery required dedicating a large real estate of the capsule; they also have a high risk of failure and possibility of leakage of caustic electrolytes that can cause severe corrosive injury and liquefactive necrosis. In a study performed on capsule endoscopy tests on 733 patients, malfunction of the batteries occurred in 17 cases.[23] To prevent such challenges, various passive actuation sampling mechanism approaches have been exploited by enabling the capsules to be more compact, economically viable, with fewer safety-associated issues.[15] In such designs, the capsule moves through the GI tract via peristalsis motion with an average speed of 1–2 cm min^{-1} and the samples are collected through simple passive actuations such as capillary wicking actions and pressure differentials forces.[12] In a patent application, a capsule was designed with a vacuum interior and a sealed opening. Once the patient swallows the capsule and it reaches the GI tract, the seal is dissolved and the intraluminal contents are pulled into the sampling reservoir.[24] In another study, Ross-Innes et al. introduced a compressed sampling mesh sponge encapsulated in an ingestible gelatin pill that is attached to a long string. The capsule rapidly dissolves in the stomach after being swallowed, and the sponge collects esophageal cells. The sponge with the collected samples is then retrieved out of the patients mouth for further analysis by pulling on the string.[25] Despite the simplicity of such passive sampling devices, there are still important design considerations and limiting factors that need major improvements. The first described capsule (from the patent) requires a well-sealed vacuum chamber inside the capsule which can significantly increase the complexity and assembly of the device. In the second study (by Ross-Innes et al.), the sampling mesh sponge cannot go beyond the stomach and the sponge retrieval by pulling onto the string upstream of the GI can cause discomfort for the patient. In addition, most passive sampling capsule devices lack the ability to seal and protect the collected samples after the sampling at targeted location is completed.

In this report, we demonstrate a passive 3D-printed gut sampling capsule that uses the swelling property of highly absorbent hydrogel as a milieu to collect the sampled microbiome and also provides the required mechanical actuation to close the capsule once sampling is completed. Hydrogels are composed of hydrophilic polymer networks capable of absorbing large quantities of water while maintaining their structure. This polymer network is typically crosslinked via covalent bonds, hydrogen bonds, van der Waals interactions, or physical entanglements.[26,27] Hydrogels have gained increasing interest in the medical field, specifically in areas such as regenerative medicine, tissue engineering, biofouling prevention, and drug delivery, due to their hydrophilic nature and biocompatibility.[26–33] Super-absorbent hydrogels, typically based on the polymerization of acrylic acid and acrylamide, have been shown to absorb 150–300 times their weight in most aqueous environments.[34,35] By taking advantage of the hydrogel's absorption capacity, as well as their mechanical properties, it is possible to design a non-invasive sampling device which can passively extract and secure samples taken from otherwise unreachable areas of the GI tract. As shown in Fig. 1, the sampling mechanism of the device consists of three steps. (i) As the patient swallows the capsule, a biodegradable enteric coating delays the sampling until the pill reaches the target location within the GI tact.

(ii) Once the capsule reaches the target location, the coating will degrade, allowing gut fluids with microorganisms to enter the capsule. (iii) As GI fluids enter the capsule, the dehydrated hydrogel will swell and fill the entire volume of the capsule by absorbing the sampling fluid and push the Polydimethylsiloxane (PDMS) membrane onto the sampling aperture, sealing the device effectively. The sealed capsule prevents further fluids from entering as well as leaving the device throughout the remaining GI tract. The hydrated hydrogel within the capsule provides an ideal living environment with nutrient for the sampled bacteria to survive before retrieval of the capsule. In addition, the high gas permeability of the PDMS membrane allows a natural gas exchange between the GI tract and inside the capsule which is
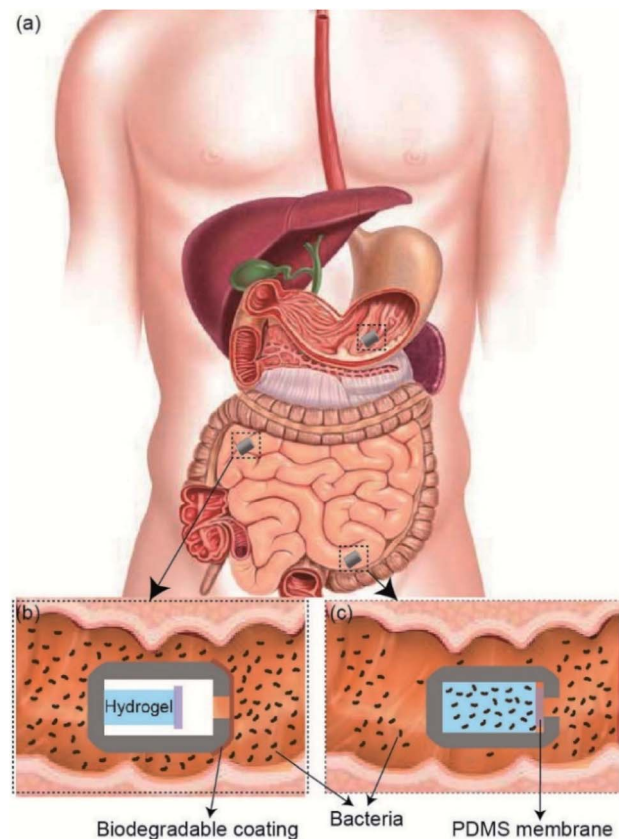
Fig. 1 (a) Schematic illustration of sampling capsule within GI tract. (b) The biodegradable coating protects the components within the capsule until it reaches the target location within the small intestine. (c) Once it reaches the target location, the biodegradable coating dissolves and allows inflow of fluids, which results in the swelling of the hydrogel and closing the sampling aperture.

essential for maintaining the natural metabolism of sampled bacteria and their survival after the capsule is sealed. The 3D-printed screw and thread on the two compartments of the capsule allows the capsule to be easily disassembled after being retrieved through excretion. The collected bacteria samples can be cultured by removing the sampling hydrogel within the device for future analysis.

Materials and methods

Device design and assembly

The detailed 3D structure of the capsule and assembled device as well as each individual component are shown in Fig. 2. The device consisted of four components: a biodegradable enteric coating, a 3D-printed housing, a sampling hydrogel, and a gas permeable PDMS membrane. The 3D-printed housing was designed with SolidWorks (Dassault Systèmes) and printed using Form 2, 3D printer through PreForm software (FormLabs) with a biocompatible methacrylate photocurable polymer *via* stereolithography. The final outer diameter and length of the printed capsule were 9 mm and 15 mm, respectively. The inner diameter and the inner length were 7 mm and 14 mm,
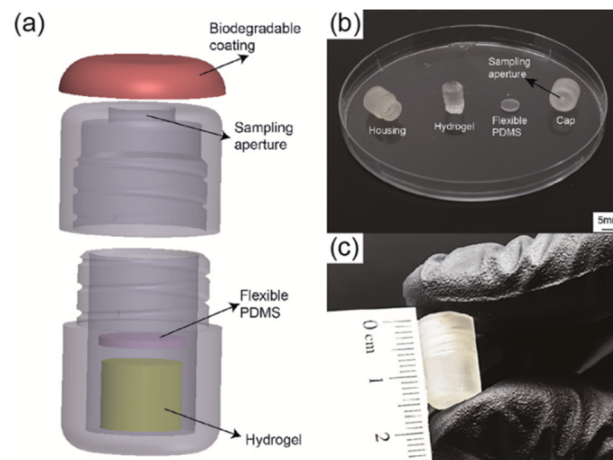

Fig. 2 (a) 3D drawing of device components including biodegradable coating, 3D printed housing, polymeric acrylic acid/acrylamide-based hydrogel, and flexible PDMS disk. (b) Photograph of individual components including 3D printed housing displaying two screw-on sections, sampling hydrogel, and PDMS disk. (c) Image of final assembled capsule.

respectively. Each capsule was designed to contain the sampling hydrogel as well as the 1 mm thick PDMS membrane placed between the hydrogel and the sampling aperture.

Fig. 2a shows a 3D rendering of the assembled device. The screwed design allowed for quick assembly and easy removal of swelled hydrogels. Fig. 2b shows an image of all components prior to assembly. The sampling aperture (5 mm in diameter) on the capsule's cap was designed to allow easy flow of fluids into the device. The highly absorbent hydrogel was synthesized with a mixture of deionized (DI) water, acrylic acid (AA) and acrylamide (AM) as monomers, methylene bis-acrylamide (MBA) as crosslinker, and ammonium persulfate (AP) as initiator. Cross-linked hydrogels were cut into cylindrical samples and fully dried before placing into the capsule. The PDMS membrane was made using a standard 1 : 10 ratio of curing agent to silicone base (Dow Corning) and cured at 80 °C for three hours, followed by laser cutting 6.5 mm in diameter circular membranes using a Class 4 CO_2 Laser (Universal Laser System). Prior to assembling of the device, a hydrophilic surface modification was performed onto the surface of the 3D-printed housing to ensure and facilitate the sampling fluid entering the capsule's aperture. Surface activation was performed by using air plasma treatment followed by poly-ethylene glycol (PEG) treatment. Plasma treatment was achieved using a Tegal Corp plasma etcher at 480 mTorr for 2 minutes, followed by submersion in a solution of PEG for 18 hours. The housing was removed from the solution, rinsed thoroughly with DI water, and allowed to air dry for 24 hours. After both the housing and the hydrogel were fully dried, devices were assembled by placing the dried hydrogel on the lower half of the 3D-printed housing. The PDMS membrane was placed between the hydrogel and the device cap. Fig. 2c shows a photograph of the final assembled capsule with a diameter of 9 mm and length of 15 mm, smaller than a standard 000 size gelatin capsule (9.97 mm × 26.14 mm).

Hydrogel synthesis and characterization

Four ratios of AA to AM were used to determine the optimum monomer mixture which resulted in the fastest absorption and highest compressive force: 10% AA/90% AM, 30% AA/70% AM, 50% AA/50% AM, 70% AA/30% AM, and 90% AA/10% AM. The total concentration of monomer mixture was 35 wt% of the total weight of the solution. DI water accounted for 60 wt% of the total weight, while MBA and AP accounted for 1 wt% and 4 wt% of the total weight, respectively. The different mixtures of AA/AM were mixed with DI water in 20 mL scintillation vials. MBA was fully dissolved by vortexing the solution for three minutes using a VWR Digital Vortex System. Once the MBA was fully dissolved, the solution was bubbled with nitrogen gas for thirty minutes in order to remove oxygen molecules which could inhibit polymerization, followed by addition of initiator. Solutions were left to polymerize at room temperature for three hours. After full polymerization, cylinders 5 mm in diameter and 12 mm in length were cut and dried in an isothermal oven overnight at 80 °C. Once hydrogels were fully dried, they were considered ready for testing. The swelling capacity of the hydrogels with different AA/AM ratio was determined by following a method similar to Zhu *et al.*[36] For each AA/AM ratio, dried samples were weighed and submerged in a solution of 1 : 10 phosphate buffer solution (PBS), purchased from Sigma Aldrich, and DI water for five hours. Samples were removed from the solution and weighed every hour to determine the amount of water absorbed. In order to determine whether the hydrogels could exert enough force to overcome the GI pressure and seal the capsule efficiently, the compressive force of each hydrogel upon swelling was measured using an Admet Tensile Tester. Dry hydrogels were placed in 10 mL scintillation vials and fixed vertically on the stage of the tensiometer. A probe with a PDMS membrane used in the capsule was attached to a 10 N load cell and placed 1 mm away from the surface of each dehydrated hydrogel block. Vials were then filled with a 1 : 10 PBS/DI water solution and the compressive force generated by each sample was measured and recorded as the hydrogel swelled and pressed against the probe over time.

Enteric coating for targeted sampling

The performance of a Cellulose Acetate Phthalate (CAP) as a pH-dependent enteric coating for controlled sampling within the small intestine was tested. CAP was obtained from G. M. Chemie Pvt. Ltd. in powder form. A thin CAP film was casted by drop-casting 10 μL of solution, consisting of 4 g of CAP dissolved in 18 mL of acetone, onto the sampling aperture of three capsules. Capsules were separately exposed to conditions simulating those found along the digestive system. One capsule was immersed in a solution of pH 7.0 for 1 minute, mimicking the pH of saliva in the mouth when the patient swallows the capsule. The second capsule was submerged in a solution of pH of 3.0 for 3 hours, imitating the gastric acidic condition. The third capsule was immersed in a solution with pH of 7.0 for 3 hours, simulating the pH of small intestine.[37] Solutions of pH 7.0 were prepared by mixing 100 mL of 0.1 M potassium phosphate monobasic with 58.2 mL of 0.1 M sodium hydroxide

and 41.8 mL of DI water, whereas the solution of pH 3.0 was prepared by mixing 100 mL of 0.1 M potassium hydrogen phthalate with 44.6 mL of 0.1 M hydrochloric acid and 55.4 mL of DI water.

For better visualization, solutions used to simulate the pHs of saliva, stomach, and small intestine were mixed with green, red, and blue dyes, respectively. After exposure to each condition, the sampling aperture of each capsule as well as the hydrogel within were shown for further analysis.

Leak test

In order to test the sealing mechanism, two independent leak tests were performed. The first test examined the electrical conductivity (EC) changes over time to detect possible leaks from the capsule after being activated and sealed with the swollen hydrogel. For this test, a fully assembled capsule and a bare hydrogel, were submerged in a 1 M solution of sodium chloride and DI water for 18 hours to ensure complete swelling of the hydrogels in both settings. They were then introduced into separate 20 mL solutions of fresh DI water and the change in electrical conductivity was measured for 6 hours using a GW Instek LCR-821 meter. Given the low conductivity of DI water (0.05 μS cm^{-1}), any significant increase in conductivity was attributed to the exchange of fluids between the DI water and the salt-infused hydrogels. In the second test a fully assembled capsule and a bare hydrogel, were placed into a solution of DI water containing red food coloring dye for 18 hours to ensure complete swelling and absorption of the food coloring dye into both hydrogels. They were then removed and placed into separate containers with DI water without opening the sealed capsule. 100 μL samples were collected from both conditions every hour and their optical absorbance peaks were detected using a BioTek Epoch™ 2 microplate spectrophotometer. This test was used to assess and compare the leakage rate of the absorbed/sampled food color dye from bare swollen hydrogel and the activated and sealed smart capsule.

In vitro bacteria sampling and survival assessment

The device's ability to effectively sample bacteria was validated by introducing devices into a culture solution to simulate the gut bacterial flora in GI environment. The capsules ability to protect the sampled bacteria after activation and sealing was tested in different extreme environments that directly affect the bacterial growth and survival rate upon direct contact. For this test, three fully assembled capsules and three bare hydrogel samples, were immersed in a solution of 100% Tryptic Soy Broth (TSB, Sigma Aldrich) containing *Escherichia coli* and incubated for eight hours at 37 °C. During the incubation period, the bacteria within the culture media were captured within the hydrated hydrogel matrix inside the capsule and the bare hydrogel samples. Next, pairs of activated/sealed capsules and bare hydrogel samples were removed from the bacteria culture solution and immersed into three different solutions including PBS, 1000 μg mL^{-1} of Tobramycin (antibiotic) prepared in PBS, and bleach diluted at a 1 : 10 ratio in DI water. PBS was used as a biocompatible media and as a control experiment.

Tobramycin and bleach solutions were used to validate the effectiveness of the sealing mechanism of activated capsules in protecting the sampled bacteria against extreme hostile environments. Bare hydrogel samples with captured bacteria were used as a control to assess the survival rate of the sampled bacteria upon direct exposure to the three conditions. The capsule and bare hydrogel pairs were kept in each of the three test solutions for one hour; the samples were then removed from the solutions and the number of viable bacteria counts for each condition was assessed. The captured bacteria were extracted by un-screwing the two parts of the capsule and removing the loaded hydrogel using a sterile inoculation loop and placing it into 10 mL of 100% TSB solution. Bare hydrogel samples with captured bacteria were also transferred directly into separated 10 mL vials of TSB solution. The captured bacteria within all hydrogel samples were extracted into the TSB solution by incubating them for 20 minutes at 37 °C under mechanical agitation. The number of viable bacteria within the hydrogel samples was determined by plating the extracted solution onto TSB/Agar plates and counting the number of Colony Forming Units (CFU).

Surface characterization

Surface contact angle measurements were taken using a Ramé-Hart Model 290 F1 Advanced Goniometer on untreated samples, plasma-treated samples, and plasma + PEG-treated samples. Initial as well as receding contact angle measurements were carried out at ambient temperature by placing a ~10 μL water droplet onto the 3D printed surface before and after the different surface modifications.

The microstructure network of the produced hydrogel and its ability to capture bacteria within its porous matrix was evaluated using Hitachi S-4800 field emission scanning electron microscopy (SEM) after Au/Pd sputtering. SEM imaging was performed on bare and bacteria-captured hydrogel samples. The first hydrogel sample was placed in a solution of PBS for 8 hours, while the second hydrogel was placed into a solution of 100% TSB inoculated with *E. coli*. Both hydrogel samples were freeze dried using a LyoStar 3 Freeze-dryer from SP Scientific for 18 hours prior to performing the SEM imaging.

Results and discussion

Surface wettability

In order to ensure a continuous pull of fluid from the gut into the narrow sampling aperture on the capsule, it was necessary to modify the capsule's polymeric surface with a long-lasting hydrophilic coating. Fig. 3 shows the results of the contact angle measurements and its stability over time on the 3D-printed capsule casing before and after different surface modification procedures of only plasma treatment and plasma treatment followed by PEG coating. Untreated 3D-printed surfaces exhibited a relativity high water contact angle with an angle of 80°. The results from the plasma treated samples show a decrease in the water contact angle right after plasma activation from 80° to 33° which implies the generation of
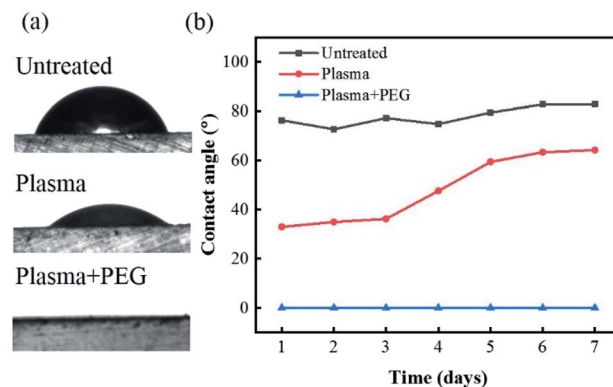

Fig. 3 (a) Image of 10 μL DI water droplet on untreated, plasma treated and plasma + PEG treated surfaces. (b) Plot of contact angle measurements for untreated, plasma treated, and plasma + PEG treated surfaces over 7 day period.

a hydrophilic surface. However, despite an initial increase in hydrophilicity, the results showed that the surface modification was unstable, and the contact angle increased from 33° to 60° after five days. On the other hand, the plasma treatment followed by the PEG coating showed a super-hydrophilic surface characteristic with a contact angle of almost 0° during the entire seven-day period. The significant decrease in contact angle and its high stability over time denotes the robustness of plasma + PEG surface modification treatment will ensure the gut fluids to easily wick and flow through the sampling aperture.

Hydrogel swelling and force profiles

The swelling response of hydrogels with different monomer ratios of 10% AA/90% AM, 30% AA/70% AM, 50% AA/50% AM, 70% AA/30% AM, and 90% AA/10% AM is shown in Fig. 4. Fig. 4a shows pictures of a fully dried and a fully swollen hydrogel. The response is expressed in terms of weight ratios calculated by dividing the difference between the weight after submersion and the initial weight of the dry sample $(G_t - G_0)$ by the initial weight (G_0). The general trend shown in Fig. 4b suggests that, with higher ratios of AA to AM, the swelling potential of hydrogels decreases. It was proved that samples with a ratio of 10% AA/90% AM, had the fastest and largest swelling potential, reaching 2.2 times their initial dry weight within 5 hours. The only exception to this trend is found in samples with a ratio of 90% AA/10% AM. These samples initially show a rapid absorption, similar to the samples of 10% AA/90% AM ratio. However, despite their rapid initial response, the swelling ratio plateaus within the first hour. The normal baseline pressure within the lumen of the human colon is reported to be between 12 mmHg and 20 mmHg, which can also reach up to 26 mmHg (3466.38 N m^{-2}) after a meal in patients with constipation.[38] Using force–pressure relations, the estimated extreme back force that can be exerted by the intra-luminal pressure in the small intestine on the PDMS membrane inside the capsule is equal to 0.46 N. Therefore, it was necessary for the PDMS membrane valve on the sampling capsule to withstand back pressures greater than 0.46 N for perfect sealing after sampling/activation. Fig. 5 shows two images of dry and
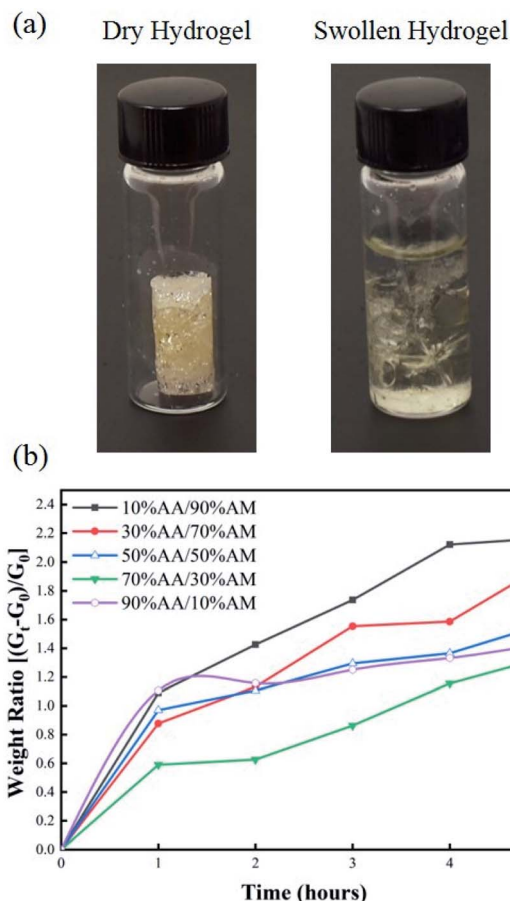
Fig. 4 (a) Image of 10% AA/90% AM hydrogel before and after swelling in PBS for 5 hours. (b) Plot of swelling ratio over time for hydrogels made with different AA/AM ratios.

Fig. 5 (a) Image of dry hydrogel (left) and swollen hydrogel (right) against force probe on tensile testing machine. Dry hydrogels were places 1 mm away from force probe. (b) Plot of force profile generated during the swelling process of hydrogels synthesized using different AA/AM ratios.

swollen hydrogels against the force probe as well as the force profile that was recorded during the hydration process of hydrogel samples made with different AA/AM ratios as a function of time. The results show that the samples with a lower AA/AM ratio show a relatively faster increase in the force exerted on the PDMS membrane. Except for the hydrogel made with the 90% AA/10% AM monomer ratio, all other hydrogels were able to provide the necessary force during a five-hour hydration and swelling period, that overcomes the estimated back pressure within the lumen of the GI tract (>0.46 N). Samples made of 10% AA/90% AM show the fastest increase, meeting the required force within an hour of hydration and swelling. The observed delay in force generated with different AA/AM ratios can be directly correlated to their corresponding swelling profiles. As seen in Fig. 5a, dry hydrogels were placed 1 mm away from the force probe, as this was the total length the hydrogels would have to swell in order to seal the capsule. The faster absorption rate translates to faster detection of force generated as the hydrogel more readily reaches the probe. Given these results, crosslinked hydrogels with the monomer ration of 10% AA/90% AM had the most suitable actuation and sampling capability, as it provided both the highest absorption and force generating properties and therefore was used in the final assembly of the sampling capsule and for further characterization.
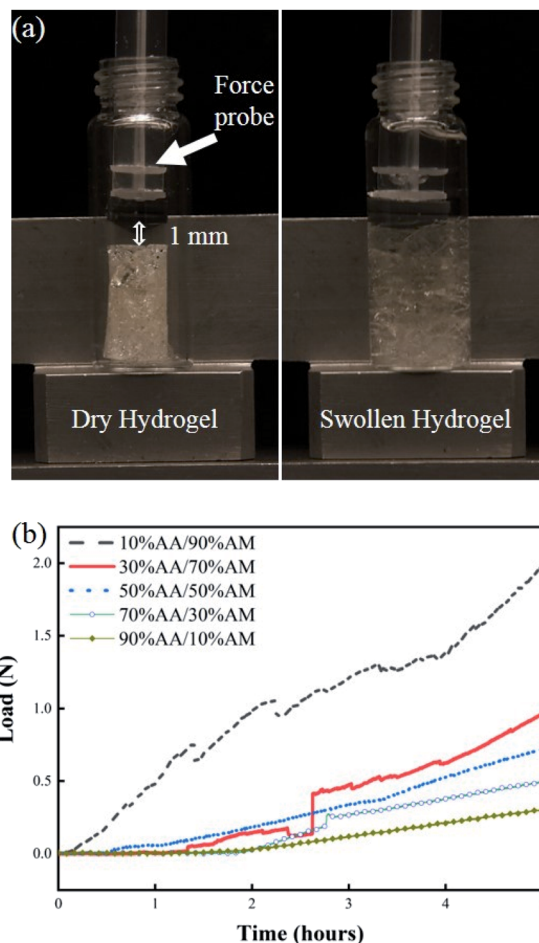
Enteric coating characterization

Ensuring that hydrogels within the capsule will only capture samples at the target location is crucial based on two reasons. First, any exposure prior to the target location can result in contamination due to unintended sampling of microorganisms from the mouth or stomach. Second, as the capsule travels through the stomach, absorption of gastric acid can create a hostile environment within the hydrogel matrix for further sampling. In order to enable selective sampling mechanism, an enteric coating which dissolves above a certain pH threshold was utilized. Due to the variability in pH along the digestive tract, several polymers have been designed for targeted drug delivery in the small intestine and colon. Among these polymers, CAP has been frequently used due to its availability, ease of synthesis, and excellent pH-dependent solubility.[42–45] CAP selectively dissolves at pH levels greater than 5.0, making an ideal polymer for an enteric coating in this application.

Fig. 6 demonstrates the performance of enteric coating towards different pH levels along with sampling visualization within the small intestine condition. Once the caps are coated
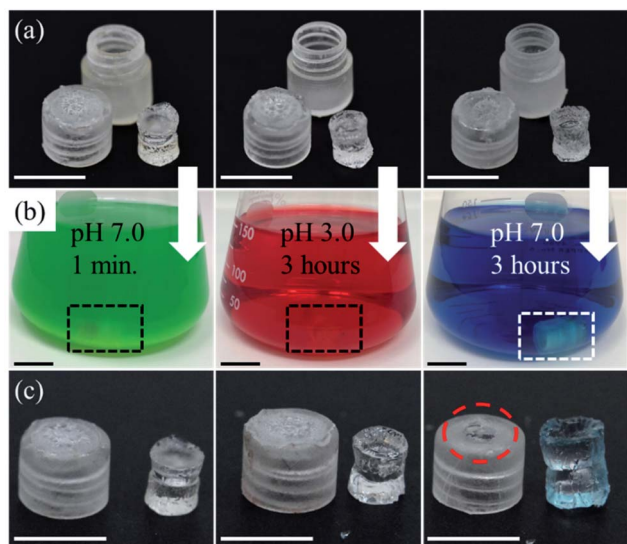
Fig. 6 (a) Images of individual device components before introduction into solutions of variable pH. The CAP coating is visible on the sampling aperture of each cap. (b) Images of assembled device inside solutions of different pH for different time lengths. Green solution simulates saliva (pH 7.0 for 1 minute), red solution simulates gastric acid (pH 3.0 for 3 hours), and blue solution simulates intestinal fluid (pH 7.0 for 3 hours). (c) Images of sampling aperture and hydrogel after exposure. As shown, the coatings of the caps associated with saliva and gastric acid remained intact, however, the enteric coating of the intestinal fluid fully dissolved which caused the hydrogel to absorb the blue dye. Scale bar 6 mm.

with a thin layer of the enteric coating, they are immersed in different pH levels including pH 7.0 (saliva/mouth), pH 3.0 (stomach), and pH 7.0 (small intestine) all of which simulate the pH levels of the GI tract as the capsule travels ahead. The images on Fig. 6a show the capsule body, hydrogel and the degradable enteric coating entirely covering the sampling aperture of each individual device before exposing the capsule to different pH buffer solutions. Different food coloring dyes including green, red, and blue were added to the buffer solutions to better visualize the saliva, stomach, and small intestine, respectively (Fig. 6b). If a hydrogel was to be exposed to the surrounding media as a result of degradation of the enteric coating, a visible change in color should be observed. Fig. 6c clearly exhibits the cap of each device as well as the hydrogel after exposure to each solution. The CAP coating as well as the hydrogels exposed to solutions of pH 7.0 for 1 minute (green) and pH 3.0 for 3 hours (red) display no signs of degradation, dissolution, swelling, or change in color. However, the coating on the sampling aperture of the device exposed to pH 7.0 for 3 hours (blue) shows vivid signs of degradation and dissolution resulting in a clear absorbance and swelling which is obvious by the distinct change in size and color. These results suggest that by utilizing a polymer with pH-dependent solubility as a degradable coating, selective targeted sampling of the small intestine is achievable.

Leak test

Once samples are collected at the targeted location within the GI, it is important that the sealing mechanism effectively prevents any further exchange of fluids to occur as it travels

further down the digestive system. Any fluid exchange beyond the target location will result in contamination of the collected sample of microbial colonies. Fig. 7a shows the experimental setup of the EC-based leak test. Any exchange between the hydrogels loaded with a 1 M solution of NaCl and the DI water would be reflected as an increase in the conductivity of the environment. Fig. 7b shows changes in conductance for a solution of undisturbed DI water, DI water after exposure to a bare hydrogel, and DI water after exposure to a sealed capsule. The baseline conductance of DI water is close to 0.5 μS, due to the lack of ions in the solution. The conductance of the media, as the bare hydrogel is introduced, increases rapidly due to the quick exchange of fluids between the hydrogel and the environment. This scenario simulates a complete failure of the sealing mechanism, where free sodium and chloride ions are released into the fresh media, thus increasing the conductance of the system. The results for the hydrogel within the capsule indicate no increase in conductance over 8 hours, suggesting there is no leak from the capsule into the fresh media.

Additionally, the results from the UV-visible spectroscopy measurements show changes in absorption intensity at different wavelengths over time. Fig. 8a shows the experimental
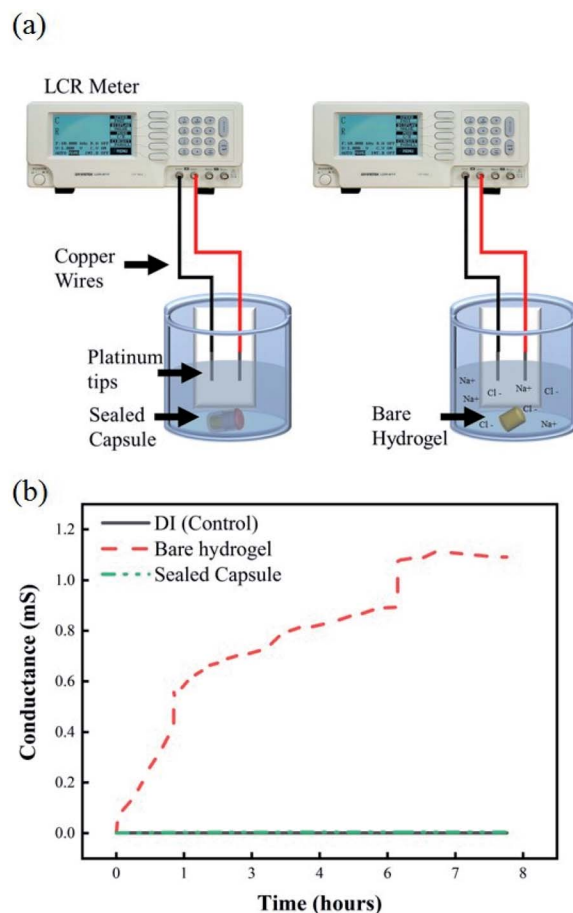

Fig. 7 (a) Experimental setup for EC-based leak test, including copper wires with platinum tips in DI water exposed to bare hydrogels and activated capsules. (b) Plot of changes in electrical conductivity for pure DI water, bare hydrogels in DI, and sealed capsules in DI.
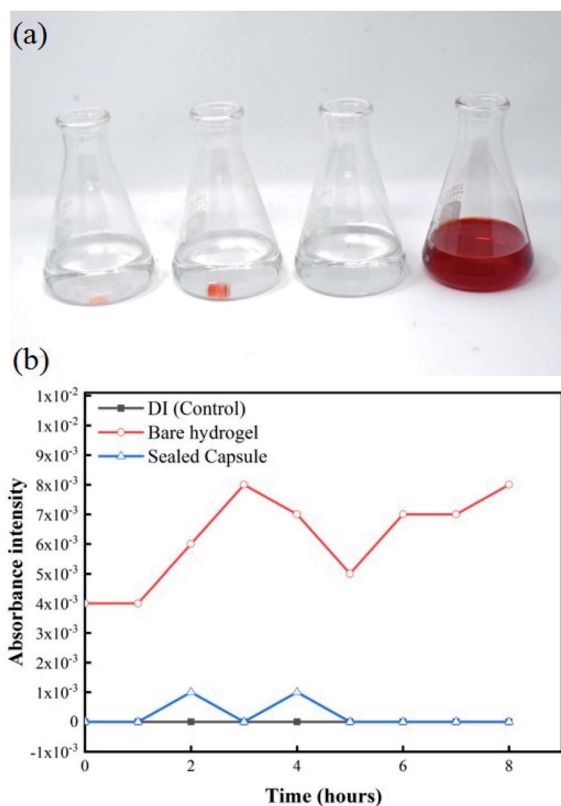
Fig. 8 (a) Experimental setup of leak detection experiment based on changes in absorption intensity of DI water exposed to bare hydrogels and hydrogels within sealed capsules carrying red food coloring dye. (b) UV spectroscopy measurements for all samples at 520 nm over 8 hour period.

setup for this test. From left to right, flasks contain a bare hydrogel in DI water, a sealed capsule in DI water, plain DI water, and DI water with red food coloring dye. The difference between the bare hydrogel and the sealed capsule becomes apparent when comparing both solutions. A slightly visible change in color can be observed in the first container as the bare hydrogel releases its contents into the solution. The solution containing the sealed capsule is similar to plain DI water, as the sealing mechanism prevents any leakages. UV-visible spectroscopy measurements for pure DI water, sealed capsule in DI, and the bare hydrogel in DI over time at a 510 nm wavelength are shown in Fig. 8b. These results confirm that the sealing mechanism prevents any leakages within 8 hours. The absorption intensity of DI water with the bare hydrogel increases over time as the food coloring is released into the environment. A dramatic increase after 5 hours confirms the presence of the dye. The absorption intensity of DI with a sealed capsule and pure DI water are comparable and remain stable over time, confirming no exchange of fluids between the hydrogel within the sealed capsule and the environment.

Bacteria sampling and retrieval assessment

Besides testing the effectiveness of the sealing mechanism, it was crucial to assess the hydrogel's ability to collect bacteria and

determine whether culturing of retrieved bacteria is achievable. The most relevant applications of this device include its ability to access currently non-accessible regions of the GI tract to collect live bacterial samples for subsequent culturing. It is not only important to determine whether further fluid exchange will occur once ingested, but also to determine whether bacteria can survive once collected. To determine bacteria sampling effectiveness and to understand the mechanism in which the hydrogel can collect microbes, cross section SEM images of the hydrogels were taken. Fig. 9 shows SEM images of the cross-sectional morphology of freeze-dried hydrogels submerged in a solution of DI water and hydrogels submerged in 100% TSB inoculated with *E. coli*. Images at low magnification show a dense network of crosslinked AA and AM monomers, with pores ranging from 10 μm to 50 μm in diameter. Fig. 9b exhibits the clean surface of a hydrogel after being swollen in DI water. Fig. 9c shows the presence of bacteria on the surface of the hydrogel submerged in a bacterial solution. These images confirm that *E. coli* were able to attach onto the solid polymer network of the hydrogel. The high porosity of the developed super absorbing hydrogels allows the bacteria-containing fluids to flow through its matrix as well as easy entrapment within the bound fluid in the hydrogel. In order to further test the capsule sealing mechanism's effectiveness after sampling, hydrogels were allowed to swell in bacteria-rich solutions and then introduced into solutions containing PBS, 1000 μg mL^{-1} Tobramycin, and bleach. Tobramycin (antibiotic) and bleach were used to simulate extreme harsh conditions which test the PDMS membrane's suitability to protect the collected bacteria from contamination. Fig. 10 shows viable bacterial counts in CFU mL^{-1} for bare hydrogels and hydrogels within sealed sampling capsules exposed to these solutions. The aim of this experiment is to characterize the effectiveness of the sealing mechanism to protect the contents of a hydrogel containing bacterial sample in a fully assembled sealed device while being exposed to these three solutions. As observed in Fig. 10 the culture results from the bare hydrogels had overall lower number
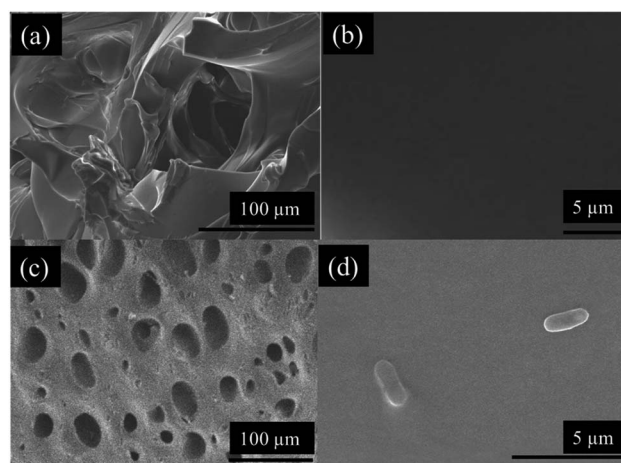

Fig. 9 (a and b) SEM images of freeze-dried hydrogels exposed to pure DI water and (c and d) TSB/PBS solutions inoculated with *E. coli*. Surface images of hydrogels exposed to bacterial solutions show that bacteria can attach to the polymer matrix.

of extractable and viable bacteria as compared to the bacteria that were extracted from hydrogels within the sealed capsules across all conditions. For hydrogels submerged in PBS, the number of CFU mL^{-1} drops three orders of magnitude when comparing bare hydrogels and hydrogels within the sealed capsule. PBS is commonly used as media for long-term storage of bacteria due its biocompatibility and preservative properties.[39] Based on this result, there is a decrease in bacterial concentration due to dilution of the initial sample collected with the bare hydrogel as it is introduced to a different solution. Despite any decrease due to dilution, there is a more obvious decline in bacterial concentration in hydrogels immersed in a solution containing Tobramycin and bleach. The number of CFU mL^{-1} drops six orders of magnitude, twice the decrease in PBS, when introduced to Tobramycin. Tobramycin, which is an aminoglycoside antibiotic, can inhibit 92% of *E. coli* strains at concentrations as low as 6.25 μg mL^{-1}.[40] Based on the inhibitive capacities of Tobramycin, the steep decline in bacterial concentration is expected. At the same time, the higher concentration of bacteria from hydrogels within the sealed capsule suggests that the sealing mechanism protected the hydrogel from interacting with the antibiotic, as well as suggesting that the hydrogel provides a hospitable environment for bacterial concentrations to remain for long periods of time. The results for hydrogels in bleach further confirm the seal's efficacy as well as the hydrogel's biocompatibility. Bleach is a strong sterilizing chemical, which is able to completely kill most bacterial strains within 10 minutes of exposure.[41] The potent antimicrobial properties of bleach inhibited microbial growth to the point where no bacterial colonies were observable on culture plates, Fig. S1 (ESI†). The fact that the bacteria within the sealed capsule are able to survive such a harsh environment supports the capsule's ability to protect samples held within the hydrogel in less harsh environments in the digestive tract. By readily collecting samples from the GI and being able to protect the microbial samples within their matrix, using a fast absorbing hydrogel proves an effective sampling agent for this device.
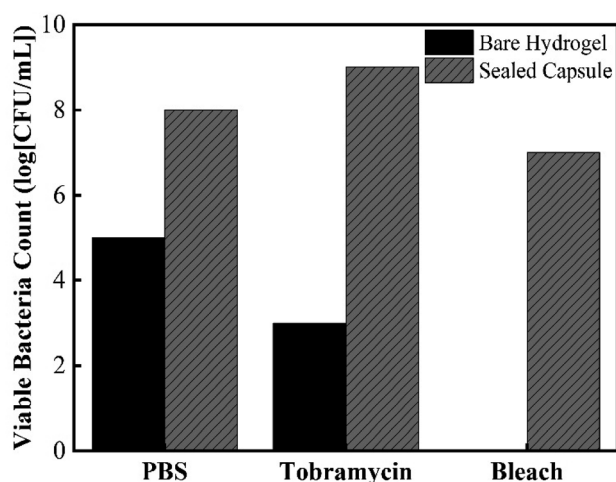
Further evidence for the hydrogel's ability to host different bacterial strains in both aerobic and anaerobic conditions is found in the results of Fig. S2, in the ESI.† The simple design and passive sampling/sealing mechanism allows for low-cost manufacturing and easy reproducibility. This in turn results in an accessible tool for sampling currently non-accessible sections of the GI tract, which will further develop our understanding of how the gut microbiota can be used as an indicator of health.

Conclusions

This study describes the use of a 3D-printed capsule, a super-absorbing hydrogel, and a PDMS membrane as a sampling device for otherwise inaccessible regions in the small intestine. The device is capable of sampling bacteria found within the GI tract by taking advantage of the hydrogel's absorbing potential and optimal mechanical properties. By modifying the surface through a plasma + PEG treatment, the surface energy of the material surrounding the sampling aperture was increased to enable stable and effective flow of fluid from the gut into the capsule. Swelling profiles for different AA/AM ratios showed that using a 10% AA/90% AM results in the most optimal swelling, absorbing twice their dry weight within the capsule's active window. Swelling and force profile characterizations of different hydrogels showed that 10% AA/90% AM ratios resulted in the most suitable sampling agents to collect fluids from the GI tract and effectively seal the device within the 1 hour sampling window of the activated capsule. Bacterial culture tests further proved the seal's efficacy of the capsule in protecting samples within the hydrogel while also showing the hydrogels ability to sustain microbial samples over time. Cultures from hydrogels within sealed capsules showed significantly higher numbers of CFU mL^{-1} compared to bare hydrogels, even when exposed to extremely harsh conditions. Bleach, the strongest antimicrobial agent tested, completely eradicated the bacteria within the bare hydrogel, while the sealed capsule was able to protect the collected bacteria yielding concentrations in the order of 10^7 CFU mL^{-1}. Further work should focus on developing a variety of biodegradable coatings which can enable sampling at target locations as well as *in vivo* testing using animal models.

Conflicts of interest

There are no conflicts to declare.

Acknowledgements

References

1 C. C. Cowie, K. F. Rust, E. S. Ford, M. S. Eberhardt, D. D. Byrd-Holt, C. Li, D. E. Williams, E. W. Gregg, K. E. Bainbridge, S. H. Saydah and L. S. Geiss, *Diabetes Care*, 2009, **32**, 287–294.

Fig. 10 Number of viable bacteria that were retrieved from sampled bacteria within bare hydrogel and sampling capsules after exposure to PBS, Tobramycin, and bleach.

2 F. Bäckhed, *Nutr. Rev.*, 2012, **70**, S14–S17.

3 A. B. Tehrani, B. G. Nezami, A. Gewirtz and S. Srinivasan, *Neurogastroenterol. Motil.*, 2012, **24**, 305–311.

4 K. Harris, A. Kassis, G. Major and C. J. Chou, *J. Obes.*, 2012, **2012**, 1–14.

5 A. Everard and P. D. Cani, *Best Pract. Res., Clin. Gastroenterol.*, 2013, **27**, 73–83.

6 R. D. Heijtz, S. Wang, F. Anuar, Y. Qian, B. Björkholm, A. Samuelsson, M. L. Hibberd, H. Forssberg and S. Pettersson, *Proc. Natl. Acad. Sci. U. S. A.*, 2011, **108**, 3047–3052.

7 J. A. Foster and K.-A. McVey Neufeld, *Trends Neurosci.*, 2013, **36**, 305–312.

8 A. Naseribafrouei, K. Hestad, E. Avershina, M. Sekelja, A. Linløkken, R. Wilson and K. Rudi, *Neurogastroenterol. Motil.*, 2014, **26**, 1155–1162.

9 E. A. Mayer, D. Padua and K. Tillisch, *BioEssays*, 2014, **36**, 933–939.

10 Y. Song, C. Liu and S. M. Finegold, *Appl. Environ. Microbiol.*, 2004, **70**, 6459–6465.

11 R. K. Clark, *Anatomy and Physiology: Understanding the Human Body*, Jones & Bartlett Learning, 2005.

12 P. Valdastri, M. Simi and R. J. Webster, *Annu. Rev. Biomed. Eng.*, 2012, **14**, 397–429.

13 P. Jesudoss, A. Mathewson, K. Twomey, F. Stam and W. M. D. Wright, *IEEE Int. Reliab. Phys. Symp. Proc.*, 2011, 3B.3.1–3B.3.7.

14 A. Moglia, A. Menciassi, P. Dario and A. Cuschieri, *Nat. Rev. Gastroenterol. Hepatol.*, 2009, **6**, 353–361.

15 Y. Amoako-Tuffour, M. L. Jones, N. Shalabi, A. Labbé, S. Vengallatore and S. Prakash, *Crit. Rev. Biomed. Eng.*, 2014, **42**, 1–15.

16 C. M. Caffrey, O. Chevalerias, C. O'Mathuna and K. Twomey, *IEEE Pervas. Comput.*, 2008, **7**, 23–29.

17 P. Jesudoss, A. Mathewson, K. Twomey, F. Stam and W. M. D. Wright, *IEEE Int. Reliab. Phys. Symp. Proc.*, 2011, 3B.3.1–3B.3.7.

18 A.-M. Singeap, C. Stanciu and A. Trifan, *World J. Gastroenterol.*, 2016, **22**, 369–378.

19 W. H. Crosby, U. S. Army and H. W. Kugler, *Am. J. Dig. Dis.*, 1957, **2**, 236–241.

20 S. Park, K. Koo, S. M. Bang, J. Y. Park, S. Y. Song and D. 'Dan' Cho, *J. Micromech. Microeng.*, 2008, **18**, 25032.

21 B. J. Prout, *Gut*, 1974, **15**, 571–572.

22 J. Cui, X. Zheng, W. Hou, Y. Zhuang, X. Pi and J. Yang, *Telemed. J. e Health*, 2008, **14**, 715–719.

23 E. Rondonotti, J. M. Herrerias, M. Pennazio, A. Caunedo, M. Mascarenhas-Saraiva and R. de Franchis, *Gastrointest. Endosc.*, 2005, **62**, 712–716.

24 I. H. H. Gu, C. St, W. Haven and H. Liang, *US Pat.*, US5971942A, 1999.

25 C. S. Ross-Innes, I. Debiram-Beecham, M. O'Donovan, E. Walker, S. Varghese, P. Lao-Sirieix, L. Lovat, M. Griffin, K. Ragunath, R. Haidry, S. S. Sami, P. Kaye, M. Novelli, B. Disep, R. Ostler, B. Aigret, B. V North, P. Bhandari, A. Haycock, D. Morris, S. Attwood, A. Dhar, C. Rees, M. D. D. Rutter, P. D. Sasieni, R. C. Fitzgerald and on behalf of the B. S. Group, *PLoS Med.*, 2015, **12**, e1001780.

26 Y. Qiu and K. Park, *Adv. Drug Delivery Rev.*, 2012, **64**, 49–60.

27 L. R. Feksa, E. A. Troian, C. D. Muller, F. Viegas, A. B. Machado and V. C. Rech, *Nanostructures for the Engineering of Cells, Tissues and Organs*, 2018, vol. 64, pp. 403–438.

28 J. M. Saul and D. F. Williams, *Handbook of Polymer Applications in Medicine and Medical Devices*, 2013, pp. 279–302.

29 J. Teßmar, F. Brandl and A. Göpferich, *Fundamentals of Tissue Engineering and Regenerative Medicine*, 2009, vol. 101, pp. 495–517.

30 S. Nejati, S. A. Mirbagheri, D. M. Warsinger and M. Fazeli, *J. Water Process Eng.*, 2019, **29**, 100782.

31 R. Rahimi, S. Shams Es-haghi, S. Chittiboyina, Z. Mutlu, S. A. Lelièvre, M. Cakmak and B. Ziaie, *Adv. Healthcare Mater.*, 2018, **7**, 1800231.

32 H. Jiang, M. Ochoa, J. F. Waimin, R. Rahimi and B. Ziaie, *Lab Chip*, 2019, **19**, 2265–2274.

33 P. Mostafalu, A. Tamayol, R. Rahimi, M. Ochoa, A. Khalilpour, G. Kiaee, I. K. Yazdi, S. Bagherifard, M. R. Dokmeci, B. Ziaie, S. R. Sonkusale and A. Khademhosseini, *Small*, 2018, 1703509.

34 S. Awasthi and R. Singhal, *J. Appl. Polym. Sci.*, 2011, **124**(3), 2348–2361.

35 S. Nesrinne and A. Djamel, *Arabian J. Chem.*, 2017, **10**, 539–547.

36 Q. Zhu, C. W. Barney and K. A. Erk, *Mater. Struct.*, 2015, **48**, 2261–2276.

37 V. C. Ibekwe, H. M. Fadda, E. L. McConnell, M. K. Khela, D. F. Evans and A. W. Basit, *Pharm. Res.*, 2008, **25**, 1828–1835.

38 J.-H. Chen, Y. Yu, Z. Yang, W.-Z. Yu, W. L. Chen, H. Yu, M. J.-M. Kim, M. Huang, S. Tan, H. Luo, J. Chen, J. D. Z. Chen and J. D. Huizinga, *Sci. Rep.*, 2017, **7**, 1.

39 C.-H. Liao and L. M. Shollenberger, *Lett. Appl. Microbiol.*, 2003, **37**(1), 45–50.

40 J. Dienstag and H. C. Neu, *Antimicrob. Agents Chemother.*, 1972, **1**, 41–45.

41 C. N. Jordan, J. A. DiCristina and D. S. Lindsay, *Vet. Parasitol.*, 2006, **136**, 343–346.

42 T. Garg, G. Rath and A. K. Goyal, *J. Drug Targeting*, 2014, **23**(3), 202–221.

43 K. Khoshnevisan, H. Maleki, H. Samadian, S. Shahsavari, M. H. Sarrafzadeh, B. Larijani, F. A. Dorkoosh, V. Haghpanah and M. R. Khorramizadeh, *Carbohydr. Polym.*, 2018, **198**, 131–141.

44 S. Mandal, K. Khandalavala, R. Pham, P. Bruck, M. Varghese, A. Kochvar, A. Monaco, P. Prathipati, C. Destache and A. Shibata, *Polymers*, 2017, **9**(12), 423.

45 R. Shrestha, A. Palat, A. M. Punnoose, S. Joshi, D. Ponraju and S. F. D. Paul, *Tissue Cell*, 2016, **48**(6), 634–643.